

Short Communication

## Hydrothermal Synthesis of NiS<sub>2</sub> Cubes with High Performance as Counter Electrodes in Dye-Sensitized Solar Cells

Chenle Zhang<sup>#1,2</sup>, Libo Deng<sup>#2</sup>, Peixin Zhang<sup>1,2,\*</sup>, Xiangzhong Ren<sup>2</sup>, Yongliang Li<sup>2</sup> and Tingshu He<sup>1</sup>

<sup>1</sup> School of Materials & Mineral Resources, Xi'an University of Architecture and Technology, Xi'an, Shanxi 710055, PR China

<sup>2</sup> College of Chemistry and Environmental Engineering, Shenzhen University, Shenzhen, Guangdong 518060, P. R. China

#These authors contributed equally to this work.

\*E-mail: [pxzhang2000@163.com](mailto:pxzhang2000@163.com)

Received: 7 October 2016 / Accepted: 31 October 2016 / Published: 12 April 2017

---

Electrocatalytic NiS<sub>2</sub> cubes were directly synthesized on F-doped tin oxide using a hydrothermal approach and used as counter electrode in dye-sensitized solar cells (DSSCs). The NiS<sub>2</sub> cubes displayed an excellent electrocatalytic activity in the reduction of I<sub>3</sub><sup>-</sup> showing a power conversion efficiency of 5.56%, which is close to that of the Pt-containing DSSC (7.05%). Furthermore, the NiS<sub>2</sub> cubes showed a comparable stability to Pt. This is ascribed to the low resistance to diffusion and transfer of electrolyte ions. These results suggest that the NiS<sub>2</sub> cubes prepared through a facile process is a promising substitute to Pt electrode.

---

**Keywords:** Nickel disulfide cubes; counter electrode; dye-sensitized solar cells

### 1. INTRODUCTION

DSSCs are a promising solar cell which show their advantage over the silicon-based photovoltaic devices in the low cost and flexibility of the device [1-4]. However, there are still many problems to be solved before these devices can achieve commercialization [5, 6]. The counter electrode (CE) is an important part of the DSSC. It collects electrons from the external circuit and the catalytic redox couple in the electrolyte, and ultimately regenerates the sensitizer [7, 8]. The traditional CE is fabricated by coating an F-doped tin oxide (FTO) glass with the noble metal Pt. Although this type of Pt CE is widely used because of its good chemical stability and high electrocatalytic activity [9], its high cost and limited Pt resources have restricted the development of DSSCs as well as other electrochemical energies that rely on the catalytic activity of Pt [10, 11]. Replacing the expensive Pt

with conducting polymers [12, 13], metal nitrides [14-16], oxides [17, 18], sulfides [19, 20], selenides [21, 22] and carbon-based materials [23, 24] have been proposed. Metal sulfides, such as nickel disulfide ( $\text{NiS}_2$ ), have potential application in CEs because of their efficient catalytic ability, high efficiency and remarkable stability [25, 26]. Most  $\text{NiS}_2$  nanostructures have been synthesized using hydrothermal [27], solvothermal [28] or  $\gamma$ -irradiation methods [29], and products with cubic, microspherical and dendritic morphologies have been produced. In addition,  $\text{NiS}_2$  cubes have favorable optical [29], magnetic [30] and electronic [31, 32] characteristics. However, most non-Pt CE materials are in the form of fine powders, and thus need to be mixed with binders or annealed to bond with the substrate and be used as CEs. This additional process leads to aggregation of the particles, which impedes the CE. The development of catalytic materials that can be grown directly on the substrate is of significance. For example, Ke et al. [33] obtained FTO- $\text{NiS}$  and Ni- $\text{NiS}$  CEs for use in DSSCs using an in situ hydrothermal method; the Ni- $\text{NiS}$ -DSSC exhibited an efficiency of 8.55%, which was higher than that of the FTO- $\text{NiS}$ -DSSC (7.47%) and even the FTO-Pt-DSSC (7.99%). In this work, we demonstrate that  $\text{NiS}_2$  cubes can be grown directly on the FTO substrate. In this system, the  $\text{NiS}_2$  cubes showed good contact with the substrate and the  $\text{NiS}_2$ -FTO CE had low resistance.

Our previous study demonstrated that hydrothermal synthesis is an effective method to prepare electrode material with high performance [34]. In this paper, we propose an in situ growth strategy that is low-cost, requires low temperatures and needs no post-treatment of the  $\text{NiS}_2$  cubes synthesized on the FTO substrates. Most importantly, the CEs obtained using this method revealed excellent contacts between the  $\text{NiS}_2$  and the substrate. The  $\text{NiS}_2$  sample was characterized using X-ray diffraction (XRD), Raman spectroscopy, scanning electron microscopy (SEM) and transmission electron microscopy (TEM). The results showed that the  $\text{NiS}_2$  had a cubic structure and a rough surface. The electrochemical results indicated that the  $\text{NiS}_2$ -containing DSSCs had high energy conversion efficiencies and that  $\text{NiS}_2$  is an extremely promising alternative to Pt for CEs.

## 2. EXPERIMENTAL

### 2.1 Materials

Nickel nitrate hexahydrate ( $\text{Ni}(\text{NO}_3)_2 \cdot 6\text{H}_2\text{O}$ , Aladdin), thiourea (Aladdin), ethylenediamine (Aladdin), chloroplatinic acid ( $\text{H}_2\text{PtCl}_6$ , Aladdin), iodine ( $\text{I}_2$ , Aladdin), lithium iodide (LiI, Aladdin), lithium perchlorate ( $\text{LiClO}_4$ , Aladdin), acetone, ethanol, anhydrous acetonitrile, tert-butanol, the redox electrolyte (LiI,  $\text{I}_2$ , 1, 2-dimethyl-3-n-propylimidazolium iodide, and 4-tert-butylpyridine in anhydrous acetonitrile) (OPV, China), di-tetrabutyl ammonium cis-bis(isothiocyanato)-bis-(2,2'-bipyridyl-4,4'-dicarboxylato)ruthenium(II) (N719) dye, F-doped tin oxide (FTO) glass (2 cm  $\times$  2 cm, 8  $\Omega$ /square, 80% transmittance).

### 2.2 Preparation of $\text{NiS}_2$ and Pt electrodes

First,  $\text{Ni}(\text{NO}_3)_2 \cdot 6\text{H}_2\text{O}$  (0.85 mmol, AR) and thiourea (0.85 mmol, AR) were mixed and stirred in deionized water (25 mL) for 2 h at room temperature. Then, ethylenediamine (0.05 mL) was added

and the solution was stirred for 3 h. The solution was then transferred to a 50 mL Teflon-lined autoclave vessel. Two pieces of FTO glass were cleaned by ultrasonic cleaning with ethanol and acetone and placed against the Teflon-lined wall of the autoclave vessel with the conducting side facing down. The autoclave was sealed and moved to an incubator, and the temperature was maintained at 150 °C for 24 h. The autoclave was cooled to room temperature and the electrodes were used without further processing. The Pt electrode was obtained by pyrolysis of an ethanol solution of  $\text{H}_2\text{PtCl}_6$  on FTO glass at 400 °C for 30 min [22].

### 2.3 Fabrication of DSSCs

Similar to our previous study [34], the  $\text{TiO}_2$  photoanodes were prepared using the doctor-blade method. The  $\text{TiO}_2$  films were soaked in a 0.3 mM solution of N719 (1:1 (v/v) mixed solvent of tert-butanol and anhydrous acetonitrile) for 24 h. The DSSCs were assembled with a dye-sensitized  $\text{TiO}_2$  photoanode and the CE, with the two electrodes separated with a hot-melt Surlyn film, and an  $\text{I}^-/\text{I}_3^-$  redox electrolyte composed of 0.1 M LiI and 0.05 M  $\text{I}_2$  in anhydrous acetonitrile was injected between them. The effective cell area was controlled by black masking to be 0.12  $\text{cm}^2$ .

### 2.4 Characterization

TEM, high-resolution TEM (HRTEM) and selected area electron diffraction (SAED) were performed with an FEI Tecnai G2 F30 (US) transmission electron microscope. XRD measurements were carried out with Cu  $\text{K}\alpha$  radiation ( $\lambda = 1.54 \text{ \AA}$ ) on a Bruker D8 diffractometer. SEM images were obtained on a JEOL JSM-7800F microscope. Raman spectra measurements were performed with an excitation wavelength of 514 nm on a Renishaw 81A946 instrument. The photocurrent–voltage ( $J$ – $V$ ) curves of the DSSCs were obtained under AM 1.5G simulated solar light. Tafel polarization measurements were carried out using symmetrical dummy cells (with two identical counter electrodes) on a CHI660D electrochemical workstation instrument with an apparent surface area of 0.15  $\text{cm}^2$  in dark conditions. Tafel polarization was measured with a scan rate of 10  $\text{mV s}^{-1}$ . Electrochemical impedance spectroscopy (EIS) with an apparent surface area of 0.15  $\text{cm}^2$  was measured from 0.1 to 100 kHz at 0 V bias and the AC amplitude was set at 0.01 V with symmetrical dummy cells. The EIS results were fitted with an appropriate equivalent circuit using Zview software. Cyclic voltammetry (CV) used a platinum wire as CE, the as-prepared CE as the working electrode and the Ag/AgCl electrode as reference electrode. The electrolyte was composed of 0.1 M  $\text{LiClO}_4$ , 10 mM LiI, 1 mM  $\text{I}_2$  and anhydrous acetonitrile, and samples were measured at a scan rate of 50  $\text{mV s}^{-1}$ .

## 3. RESULTS AND DISCUSSION

### 3.1 Morphology and structures

The phases of the as-prepared samples attached to the FTO glass substrates were characterized by XRD and the results are shown in Fig. 1a. The XRD patterns show strong peaks corresponding to

the FTO glass. Other peaks observed at  $27.3^\circ$ ,  $31.6^\circ$ ,  $35.3^\circ$ ,  $38.8^\circ$ ,  $45.3^\circ$ ,  $53.6^\circ$ ,  $58.8^\circ$ ,  $61.2^\circ$ ,  $74.8^\circ$  and  $83.4^\circ$  were assigned to the 111, 200, 210, 211, 220, 311, 230, 321, 420 and 422 diffraction peaks of  $\text{NiS}_2$  (JCPDS No. 11-0099) [26]. These results confirm that  $\text{NiS}_2$  was successfully grown on the FTO glass surface. The crystallite size of the  $\text{NiS}_2$  was calculated using the Scherrer formula to be approximately 37.7 nm [35].

In addition to XRD, Raman spectroscopy is also a powerful technique to analysis the crystallite structure of the sample. Fig. 1b shows the Raman spectra of the as-prepared samples. The bands at 270, 282, 480, 487, 596 and  $1000\text{ cm}^{-1}$  are assigned to the  $A_{1g}$  and  $E_g$  modes of  $\text{NiS}_2$  [36]. These results further indicate that the sample is  $\text{NiS}_2$ , and that the  $\text{NiS}_2$  does not contain impurities.

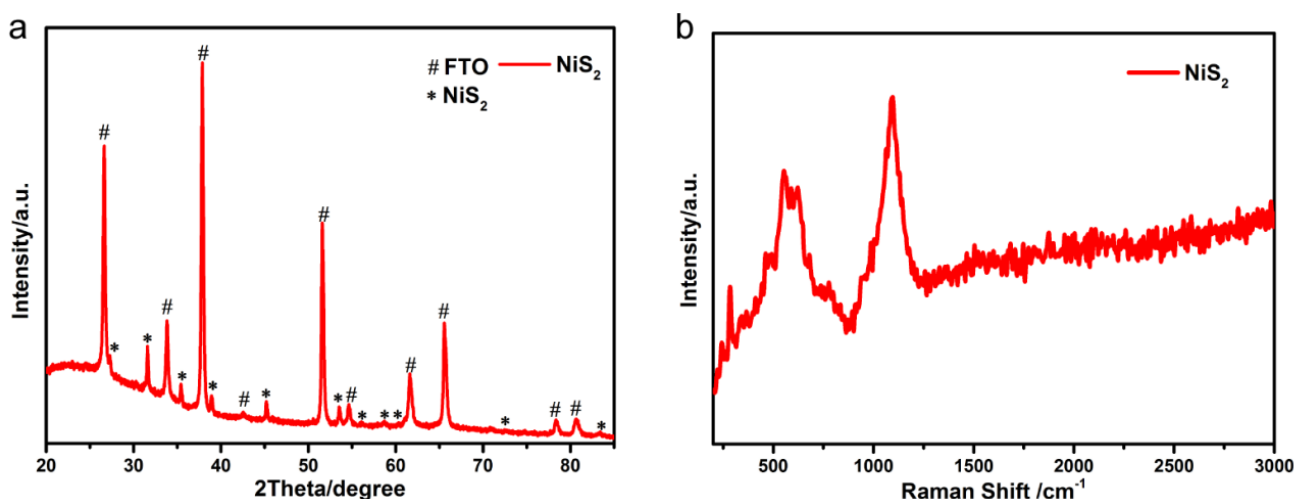


**Figure 1.** (a) XRD patterns of the  $\text{NiS}_2$  CE and (b) Raman spectra of the  $\text{NiS}_2$  CE.

SEM images were acquired to better understand the morphology of the sample. Typical low-magnification SEM images of  $\text{NiS}_2$  are shown in Fig. 2a, b, from which crystalline particles of different sizes on the surface of the FTO glass can be seen. The cubes have an average diameter of approximately  $2\ \mu\text{m}$ . These images clearly show that  $\text{NiS}_2$  cubes were successfully grown on the FTO surface using a low-temperature hydrothermal method. Furthermore, the image reveals that the surface of the  $\text{NiS}_2$  cubes is not smooth. These uneven surfaces can act as active catalytic sites and promote the electrocatalytic activity of the CE.

To further observe the inner structure of the  $\text{NiS}_2$  cube and explain these phenomena, we used TEM and SAED. These techniques provided more detailed insight into the microstructure of the sample and the images are shown in Fig. 2c, d. The TEM image in Fig. 2c indicates that the  $\text{NiS}_2$  cube is solid and has a relatively regular edge. The HRTEM image of  $\text{NiS}_2$  (Fig. 2d) shows a lattice spacing of 0.33 nm, which corresponds to the (111) plane of  $\text{NiS}_2$ . The SAED image (inset in Fig. 2d) shows that the as-prepared  $\text{NiS}_2$  cubes are highly crystalline.

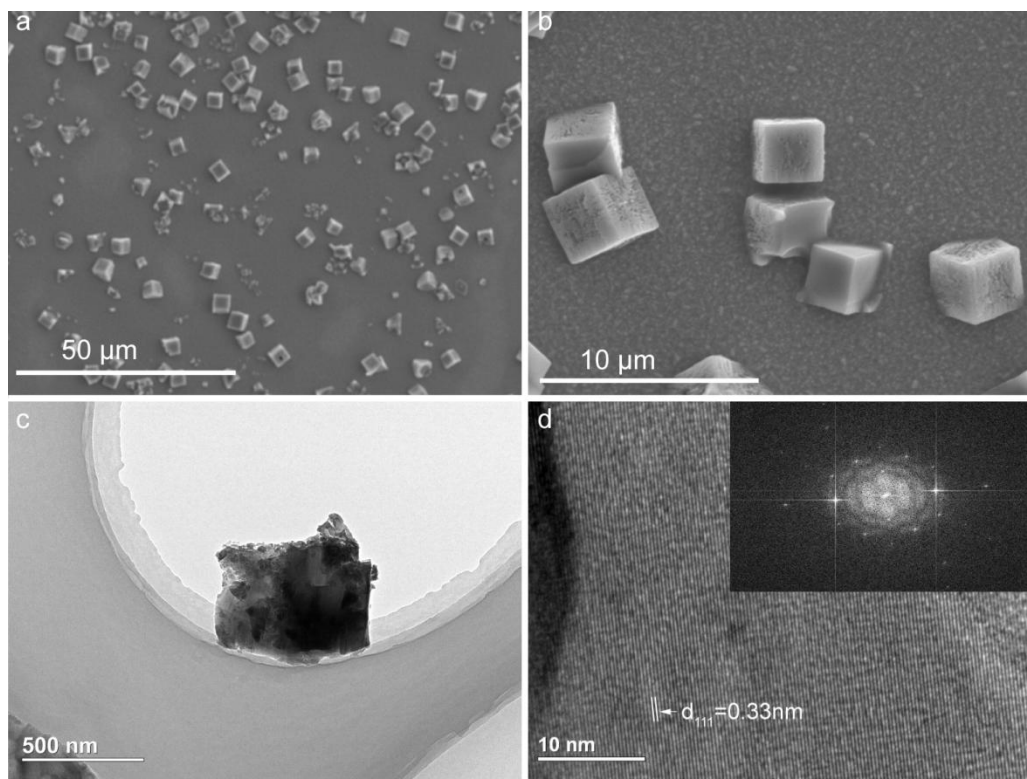
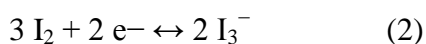


**Figure 2.** (a, b) SEM images, (c) TEM images, (d) HRTEM images and selected area electron diffraction pattern of NiS<sub>2</sub> (inset in Fig. 2d).

### 3.2 Electrochemical performance

The photovoltaic performance of DSSCs can be analysed using  $J$ - $V$  curves, shown for DSSCs containing NiS<sub>2</sub> and Pt CEs in Fig. 3a. The corresponding photovoltaic and EIS parameters are summarized in Table 1. The efficiency ( $\eta$ ) of the DSSC with the NiS<sub>2</sub> CE is 5.56%, which is close to that of the cell containing the Pt CE (7.01%). This is attributed to the increase in the fill factor (FF), the similar open circuit voltage ( $V_{oc}$ ) to that in the DSSC containing the Pt CE, the reduced interfacial resistance, and the relatively high short-circuit current density ( $J_{sc}$ ). These results were confirmed by the EIS, CV and Tafel polarization results.

To investigate the reaction kinetics and catalytic activity of the NiS<sub>2</sub> CEs, CV was measured using a three-electrode system. As shown in Fig. 3b, two redox reactions occurred and these can be assigned to reactions (1) and (2):



The catalytic activity is reflected by two parameters, the peak-to-peak separation ( $E_{pp}$ ) and the peak current [20]. A smaller  $E_{pp}$  indicates better reversibility of the redox reaction and a higher cathodic peak current density shows a faster reduction rate [37]. The cathodic peak current density for the Pt CE is slightly higher than that for the NiS<sub>2</sub> CE and the  $E_{pp}$  values for the NiS<sub>2</sub> CE are slightly higher than those for the Pt CE. The high current density of the NiS<sub>2</sub> CE results from the larger contact area and better contact of the cubic structures with the FTO glass substrate. In addition, the strong and

fast electrocatalytic reaction reflects the similar catalytic activity of the NiS<sub>2</sub> cubes as compared with Pt.

EIS experiments were carried out to evaluate the electrochemical characteristics of the CEs. The results are shown in Fig. 3c, and an equivalent circuit model is also shown in the inset of this figure. The charge transfer resistance ( $R_{ct}$ ) value of the NiS<sub>2</sub> CE was 5.23  $\Omega$ , which is higher than that of the Pt CE (3.08  $\Omega$ ). The series resistance ( $R_s$ ) value of the NiS<sub>2</sub> CE was lower than that of the Pt CE. Due to that the NiS<sub>2</sub> cubes were grown on the FTO glass, the NiS<sub>2</sub> is in good contact with the substrate. Moreover, the structure of the NiS<sub>2</sub> cubes endows them with a huge surface area, and thus the NiS<sub>2</sub> cubes provide more active sites for the reaction compared with Pt. These factors help the NiS<sub>2</sub> CE to collect electrons and drive the reaction.

Tafel polarization measurement is an efficient way to assess the electrochemical catalytic activities of CEs. The catalytic activity is reflected in the Tafel graph by two parameters: the exchange current density ( $J_0$ ) and the limiting current density ( $J_{lim}$ ). These two parameters are shown in Fig. 3d with the results of the Tafel polarization measurement. A larger slope in the anodic or cathodic branch implies a higher  $J_0$  of the CE [38]. The anodic and cathodic branches of the NiS<sub>2</sub> cubes showed smaller slopes than those of Pt, which indicates that the  $J_0$  of the NiS<sub>2</sub> cubes is smaller than that of Pt. In contrast, the  $R_{ct}$  for the as-prepared NiS<sub>2</sub> CE is greater than that for the Pt CE.

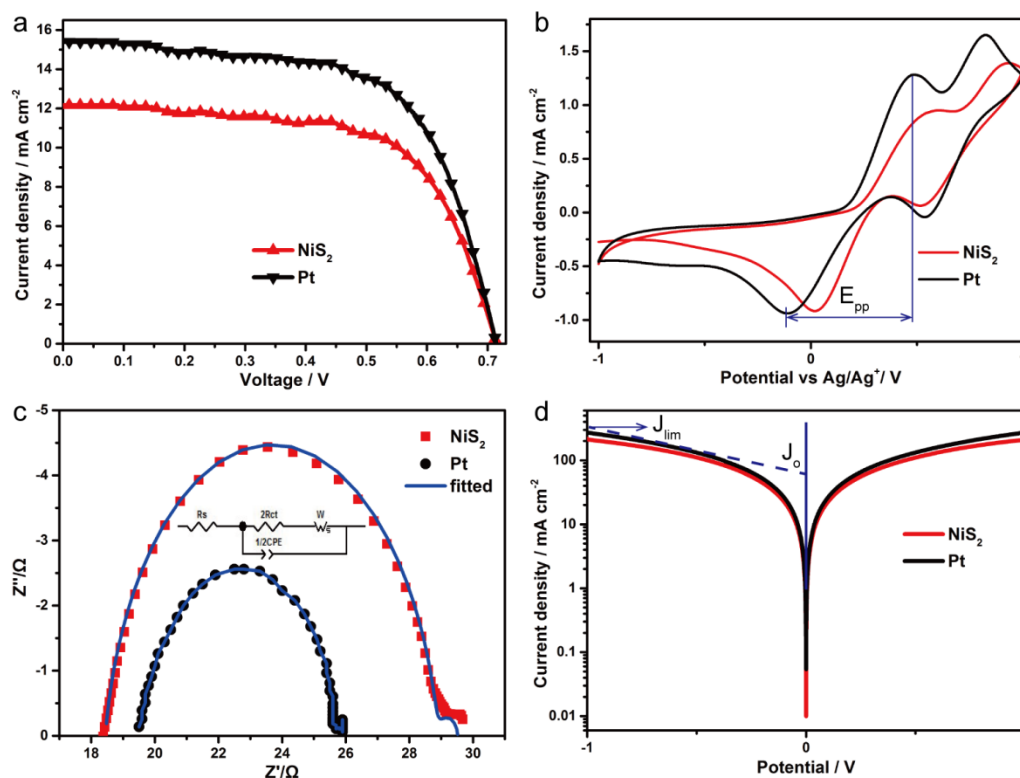


**Figure 3.** (a) Photocurrent–voltage curves, (b) cyclic voltammetry curves, (c) electrochemical impedance spectroscopy plots and (d) Tafel polarization curve of cells with different counter electrodes (NiS<sub>2</sub> (red), Pt (black)). The inset in Fig. 3c presents the equivalent circuit.

The diffusivity of the redox couple and the catalytic characteristics of the CE is determined by  $J_{lim}$  [39]. The  $J_{lim}$  of the NiS<sub>2</sub> cubes is similar to that of Pt, which means that the redox couple at the NiS<sub>2</sub> cubes has a high diffusion coefficient, and reflects the high diffusion rate of the redox couple in the electrolyte. This means that DSSCs containing NiS<sub>2</sub> CEs are expected to have relatively high photovoltaic performances.

**Table 1.** Photovoltaic parameters of the dye sensitized solar cells and simulated electrochemical impedance spectroscopy parameters of symmetrical cells fabricated using the two counter electrodes.

CE catalysts	dye	$J_{sc}$ [mA/cm <sup>2</sup> ]	$V_{oc}$ [V]	$FF$	PCE[%]	$R_s$ [Ω]	$R_{ct}$ [Ω]
NiS <sub>2</sub> cube	N719	12.16	0.714	0.64	5.56	18.44	5.23
Pt	N719	15.39	0.714	0.62	7.05	19.56	3.08

The stability of the electrodes is crucial for a powering device [40]. The DSSCs consisted of the NiS<sub>2</sub> and Pt CEs were therefore aged for 10 days, during which EIS measurement were performed to examine the stability. The results are shown in Fig. 4. It can be seen the value of  $R_s$  changed only slightly for both CEs, which means that the accumulation effect of time on the adhesion between the catalytic material and the substrate is very small. In contrast, the  $R_{ct}$  of both samples increased continuously, although the largest change was observed for the NiS<sub>2</sub> cubes after 10 days of aging. This suggests that the Pt CE has slightly better electrochemical stability than the NiS<sub>2</sub> cubes CE.

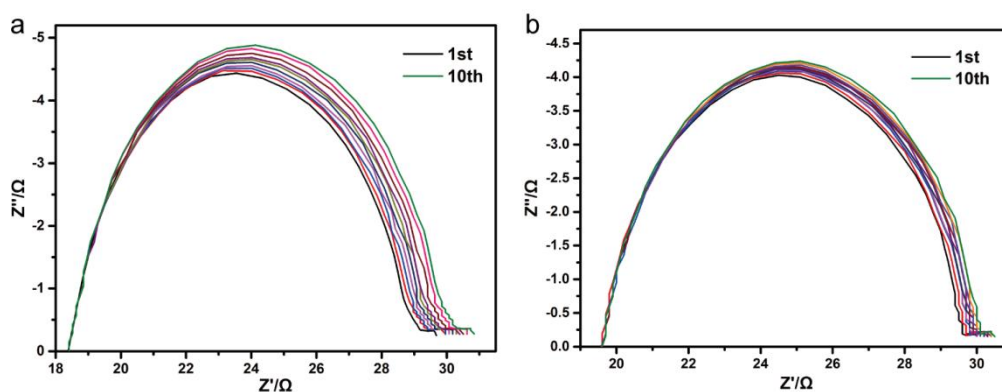


**Figure 4.** Nyquist plots for electrochemical impedance spectroscopy of (a) NiS<sub>2</sub> and (b) Pt electrodes for symmetrical cells showing the consecutive cycles of cells aged for more than 10 days.

#### 4. CONCLUSIONS

In summary, NiS<sub>2</sub> cubes were successfully synthesized using a facile one-step hydrothermal reaction on an FTO glass surface and used as CEs in DSSCs. The DSSC containing the NiS<sub>2</sub> CE demonstrated an excellent energy conversion efficiency of 5.56%, which is close to that of the DSSC

with a Pt CE (7.05%) using an iodide electrolyte system. The electrochemical results indicate that NiS<sub>2</sub> cubes are an extremely promising alternative to Pt for CEs. Furthermore, the NiS<sub>2</sub> CEs showed a comparable stability to Pt and they are easily prepared with low cost. Therefore, these electrodes might be a promising substitute to the Pt electrode.

#### ACKNOWLEDGEMENTS

This work was supported by Shenzhen Government's Plan of Science and Technology (Grants JCYJ20150324141711596 and JCYJ20160422112012739), the Natural Science Foundation of Guangdong (2015A030310087), and the National Natural Science Foundation of China (Grants #51374146, 51602202).

#### References

1. B. O'Regan, M. Grätzel, *Nature*, 353(1991) 737-740.
2. K. Kakiage, Y. Aoyama, T. Yano, K. Oya, J.I. Fujisawa, M. Hanaya, *Chem. commun.*, 51 (2015) 15894-15897.
3. H.K. Jun, M.A. Careem, A.K. Arof, *Int. J. Electrochem. Sci.*, 11 (2016) 2909-2918
4. P. Enciso, J.-D. Decoppet, T. Moehl, M. Grätzel, M. Wörner, M.F. Cerdá, *Int. J. Electrochem. Sci.*, 11 (2016) 3604-3614.
5. M. Grätzel, *Nature*, 414 (2001) 338-344
6. Y. Li, H. Wang, H. Zhang, P. Liu, Y. Wang, W. Fang, H. Yang, Y. Li, H. Zhao, *Chem. commun.*, 50 (2014) 5569-5571.
7. X. Chen, Y. Hou, B. Zhang, X.H. Yang, H.G. Yang, *Chem. commun.*, 49 (2013) 5793-5795.
8. E. Bi, H. Chen, X. Yang, W. Peng, M. Grätzel, L. Han, *Energ. Environ. Sci.*, 7 (2014) 2637.
9. Y. L. Lee, C. L. Chen, L. W. Chong, C. H. Chen, Y. F. Liu, C. F. Chi, *Electrochem. Commun.*, 12 (2010) 1662-1665.
10. Y. Li, W. Li, T. Ke, P. Zhang, X. Ren, L. Deng, *Electrochem. Commun.*, 69 (2016) 68-71.
11. L. Deng, H. Fang, P. Zhang, A. Abdelkader, X. Ren, Y. Li, N. Xie, *J. Electrochem. Soc.*, 163 (2016) H343-H349.
12. K. M. Lee, P. Y. Chen, C. Y. Hsu, J. H. Huang, W. H. Ho, H. C. Chen, K. C. Ho, *J. Power Sources*, 188 (2009) 313-318.
13. T. Makris, V. Dracopoulos, T. Stergiopoulos, P. Lianos, *Electrochim. Acta*, 56 (2011) 2004-2008
14. M. Wu, X. Lin, Y. Wang, L. Wang, W. Guo, D. Qi, X. Peng, A. Hagfeldt, M. Gratzel, T. Ma, *J. Am. Chem. Soc.*, 134 (2012) 3419-3428.
15. M. Wu, Q. Zhang, J. Xiao, C. Ma, X. Lin, C. Miao, Y. He, Y. Gao, A. Hagfeldt, T. Ma, *J. Mater. Chem.*, 21 (2011) 10761.
16. T. He, Y. Li, S. Yun, P. Zhang, C. Zhang, *J. Inorg. Mater.*, 31 (2016) 113.
17. M. Wu, X. Lin, L. Wang, W. Guo, Y. Wang, J. Xiao, A. Hagfeldt, T. Ma, *J. Phys. Chem. C*, 115 (2011) 22598-22602.
18. S. Yun, L. Wang, W. Guo, T. Ma, *Electrochem. Commun.*, 24 (2012) 69-73.
19. Y.C. Wang, D.Y. Wang, Y.T. Jiang, H.A. Chen, C.C. Chen, K.C. Ho, H.L. Chou, C.W. Chen, *Angew. Chem. Int. Ed. Engl.*, 52 (2013) 6694-6698.
20. Y. Liao, K. Pan, Q. Pan, G. Wang, W. Zhou, H. Fu, *Nanoscale*, 7 (2015) 1623-1626.
21. W. Wang, X. Pan, W. Liu, B. Zhang, H. Chen, X. Fang, J. Yao, S. Dai, *Chem. commun.*, 50 (2014) 2618-2620.
22. F. Gong, H. Wang, X. Xu, G. Zhou, Z.S. Wang, *J. Am. Chem. Soc.*, 134 (2012) 10953-10958.
23. W. Y. Cheng, C. C. Wang, S. Y. Lu, *Carbon*, 54 (2013) 291-299.

24. S. Hwang, M. Batmunkh, M.J. Nine, H. Chung, H. Jeong, *ChemPhysChem.*, 16 (2015) 53-65
25. I.A. Ji, H.M. Choi, J.H. Bang, *Mater. Lett.*, 123 (2014) 51-54.
26. J. Zheng, W. Zhou, Y. Ma, W. Cao, C. Wang, L. Guo, *Chem. commun.*, 51 (2015) 12863-12866.
27. L. Wang, Y. Zhu, H. Li, Q. Li, Y. Qian, *J. Solid State Chem.*, 183 (2010) 223-227.
28. S. L. Yang, H. B. Yao, M. R. Gao, S. H. Yu, *CrystEngComm.*, 11 (2009) 1383.
29. R. Luo, X. Sun, L. Yan, W. Chen, *Chem. lett.*, 33 (2004) 830-831
30. W. Wang, S. Y. Wang, Y. L. Gao, K. Y. Wang, M. Liu, *Mater. Sci. Eng. B*, 133 (2006) 167-171.
31. L.T. Cheng, J. Dzubiella, J.A. McCammon, B. Li, *J. Chem. Phys.*, 127 (2007) 084503.
32. Y. M. Chai, X. Shang, G. Q. Han, B. Dong, W. H. Hu, Y. R. Liu, X. Li, C. G. Liu, *Int. J. Electrochem. Sci.*, 11 (2016) 3050-3055
33. W. Ke, G. Fang, H. Tao, P. Qin, J. Wang, H. Lei, Q. Liu, X. Zhao, *ACS Appl. Mater. Inter.*, 6 (2014) 5525-5530.
34. C. Zhang, Y. Li, L. Deng, P. Zhang, X. Ren, S. Yun, *J. Solid State Electrochem.*, 20 (2016) 2373-2382.
35. P. Scherrer, *Nachr. Ges. Wiss. Göttingen*, 2 (1918) 96-100.
36. T. Suzuki, K. Uchinokura, T. Sekine, E. Matsuura, *Solid State Commun.*, 23 (1977) 847-852
37. Y. Xiao, J. Wu, J. Lin, G. Yue, J. Lin, M. Huang, Y. Huang, Z. Lan, L. Fan, *J. Mater. Chem. A*, 1 (2013) 13885.
38. Z. Li, F. Gong, G. Zhou, Z. S. Wang, *J. Phys. Chem. C*, 117 (2013) 6561-6566.
39. A. Hauch, A. Georg, *Electrochim. Acta*, 46 (2001) 3457-3466.
40. L. Deng, W. Zhang, X. Ren, P. Zhang, Y. Li, L. Sun, Y. Gao, *RSC Adv.*, 6 (2016) 78100-78105.

© 2017 The Authors. Published by ESG ([www.electrochemsci.org](http://www.electrochemsci.org)). This article is an open access article distributed under the terms and conditions of the Creative Commons Attribution license (<http://creativecommons.org/licenses/by/4.0/>).